

Microstructure and Mechanical Properties of Microalloyed Steels Containing Molybdenum

Jaqueline Polezi Mazini^{a*} , André Itman Filho^a, Breno Mendes Rabelo Ávila^a ,

Rosana Vilarim da Silva^a, Pedro Gabriel Bonella de Oliveira^b

^aInstituto Federal de Educação Ciência e Tecnologia do Espírito Santo, Programa de Mestrado em Engenharia Metalúrgica e de Materiais, Vitória, ES, Brasil.

^bUniversidade de São Paulo, Escola de Engenharia de São Carlos, Departamento de Engenharia de Materiais, São Carlos, SP, Brasil.

Received: December 5, 2021; Accepted: December 7, 2021

Microalloyed steels have a maximum of 2% in alloying elements and are used in the automotive and petrochemical industries. The microstructure and mechanical properties of these steels depend on chemical composition, processing and addition of molybdenum, niobium, titanium and vanadium. To evaluate the molybdenum effect in microstructure and mechanical properties, two microalloyed steels, with similar levels of niobium, titanium and vanadium, were prepared and forged. The steels have 0.056 and 0.160 percent by weight of molybdenum. The bars were homogenized, quenched and tempered. The specimens were machined for tensile and impact tests, hardness and microstructural analyzes by confocal and scanning electron microscopy. The ThermoCalc software was used to evaluate the carbides characteristics. The results show that steel with 0.160% Mo presents greater amount of bainite and austenite retained. It's possible that formation of carbides by the secondary hardening mechanism increase in mechanical strength and a reduction in toughness.

Keywords: *Microalloyed steel, molybdenum, API steel, ThermoCalc.*

1. Introduction

The oil and gas industry requires the development of steels that meet API 5L (American Petroleum Institute) requirements. These steels must have an excellent combination of properties, such as high mechanical strength to withstand pressure in deep water, corrosion resistance in a marine environment, toughness and adequate weldability^{1,2}.

The conventional thermomechanical process for these steels is the controlled rolling. However, forging is used in the manufacture of parts with complex geometry, such as valves for pipelines and connections for transporting gas and oil. This process allows the manufacture of parts with a wide range of dimensions and shapes, microstructure control and an excellent combination of mechanical properties, after quenching and tempering treatments³. Nowadays, several industries produce connections and accessories for use in pipelines. The forging process is also widely used in the automotive industry, as the technique produces components with adequate manufacturing cost. There is a little loss of material, as the forged product has dimensions close to the final product^{4,5}.

Associated with the forging process, the addition of niobium, titanium and vanadium at levels of up to 0.15% by weight promotes solid solution hardening and grain refinement. These elements favor the formation of finely dispersed carbonitrides in the matrix during the austenite-ferrite transformation and are effective in increasing mechanical strength and tenacity^{6,7}.

In this case, quenching and tempering heat treatments are used to control the microstructures and optimize the mechanical properties of microalloyed steels. Previous studies show that a microstructure composed of bainite, ferrite and retained austenite (M/A) is common in microalloyed steels⁸.

Regarding the molybdenum and niobium, another important effect is the reduction of the austenite-ferrite transformation temperature, which favors the formation of displacive structures, such as acicular ferrite and bainite^{8,9}. In these steels, the microstructures generally consist of a matrix with polygonal (equiaxial) ferrite grains with second phase islands that can be degenerate pearlite, bainite, martensite/retained austenite (M/A) or acicular ferrite (AF)⁶. It is possible that molybdenum has a greater effect on the finer microstructures, while niobium on the grain refining^{7,10}.

According to the literature, the microstructure with these constituents is interesting to meet API 5L standards^{6,11-13}. Previous studies showed that a steel containing 0,3 wt.% Mo produced a high volume fraction of granular bainite, with significant benefits to increase elongation after the tempering treatment^{11,12}. Regarding the carbides formed in the austenite-ferrite transformation and secondary hardening, they are difficult to be observed even in scanning electron microscopes¹⁴. In this case, computational thermodynamic simulation is an efficient tool to predict the quantity and temperature of solubilization of carbides, oxides, sulfides and nitrides^{15,16}.

In this context, this present research aims to evaluate molybdenum effect on the microstructure, hardness, mechanical

*e-mail: jaquepomezimazini@gmail.com

strength and Charpy impact tests of two microalloyed steels, with characteristics of the API 5L standard and similar levels of niobium, titanium and vanadium, after quenching and tempering at different temperatures. A qualitative analysis and the carbide stoichiometry were determined through thermodynamic simulations with the ThermoCalc software.

2. Experimental Procedures

Two microalloyed steels were manufactured in an induction furnace with a capacity of 300 kg at Fundação Grupo Metal, SP-Brazil. The liquid metal was poured into a cast iron ingot mold and the chemical compositions were determined by optical emission spectrometry.

Ingots were cut into three pieces with similar weights. These parts were heat treated to 1050 °C and forged with a square section of approximately 40 mm on the side and a length of 1500 mm. The last passes were made at a temperature of 850 °C to refine the grain. Afterwards, the bars were annealed at 930 °C for two hours to homogenize the microstructure. Figure 1 illustrates thermomechanical processing.

After cooling, samples cut in longitudinal orientation of 32x32x120 mm were prepared and austenitized at 900 °C in a muffle furnace for 120 minutes and cooled in water. This temperature corresponds to a fully austenitic region, above A_{c3} , considering the temperatures A_{c1} and A_{c3} , calculated by Kasatkin¹⁷.

Subsequently tempering was carried out at 150, 250, 350, 450, 550 and 600 °C for one hour with cooling in water. On these samples, hardness measurements were obtained, according to ASTM E18, in a Rockwell B durometer, with a load of 100 kgf, to determine the tempering curves.

Specimens under tempering conditions at 450 and 600 °C were machined for mechanical tests and microstructural analyses. These temperatures were selected according to the highest and lowest hardness values observed in the tempering curve.

After preparation by conventional metallography, the microstructures were revealed with the reagents Nital 2%

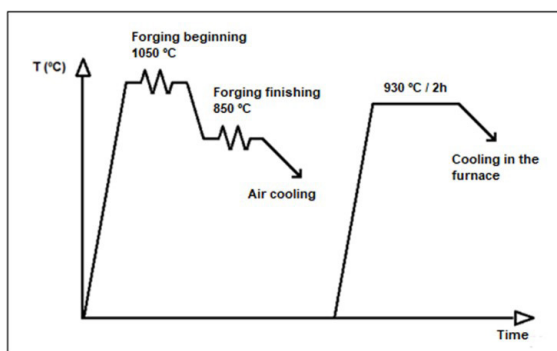


Figure 1. Thermomechanical processing of microalloyed steels.

(nitric acid 2% in ethyl alcohol) and Lepera (4% picric acid in ethanol and sodium metabisulfite 1% in distilled water) for 30 seconds. Microstructural analyzes were performed using confocal optical microscopy (MOC) and scanning electron microscopy (SEM) with an energy dispersive spectroscopy (EDS) system. Grain sizes were measured according to ASTM E112 standard.

Tensile tests were carried according to ASTM E8, in a universal machine with a 50 mm strain gauge, 25 mm measurable strain and 1 mm/min speed. The absorbed energy at impact was determined according to ASTM E23-16a standard using three specimens submitted to Charpy test at temperature of minus 20 °C. The absorbed energy at impact was determined in accordance with ASTM E23-16a with Charpy tests at a temperature minus 20 °C. The results of the traction and impact tests correspond to the averages of three specimens for each condition.

A qualitative analysis and the carbide stoichiometry were determined through thermodynamic simulations with the ThermoCalc software, considering the percentages of chemical elements, FCC basis for an matrix and temperature in the range of 200 to 1500 °C.

3. Results and Discussion

The chemical compositions of microalloyed steels are shown in Table 1. The sum of the niobium, titanium and vanadium contents are similar and meet the API 5L standard. To facilitate presentation, steels with 0.160% Mo and 0.056% Mo are called 160-Mo and 056-Mo, respectively.

Regarding microstructures, the grain sizes were 8 ± 1 and 9 ± 1 ASTM for 160-Mo and 056-Mo steels, respectively, in the annealed condition. The smaller grain in 056-Mo steel is possibly related to the higher niobium content. Javaheri observed the influence of niobium in the refinement of grains of two steels, even for a small difference in the element content, around 0.01%¹⁸. Niobium forms carbides that anchor grain boundaries during austenitization and inhibit the grain growth^{19,20}. The microstructures of the steels, after quenching at 900 °C with water cooling, are shown in Figures 2(a) and 2(b).

The bainite bundles observed in 160-Mo steel, in Figure 2(a), are elongated and may be responsible for the increase in hardness and mechanical strength⁸. It is likely that the higher molybdenum content is responsible for the reduction in the transformation temperature and favors a greater amount of elongated bainite plates²¹. Previous studies indicate that grain size can influence bainite growth with the presence of retained austenite (M/A)²². With the increase in grain size, there is a reduction in the boundary surface energy and greater difficulty in diffusive transformations. This favors adiffusional transformations such as bainite²³. Regarding the presence of M/A, this phase acts as a microcrack initiator and can reduce the toughness of the material²⁴. In Figure 2(b),

Table 1. Chemical compositions of microalloyed steels (percentage by weight).

	C	Mn	P	S	Nb	Ti	V	Cr	Ni	Mo	N
160-Mo	0.09	0.42	0.030	0.013	0.010	0.020	0.010	0.29	0.40	0.160	0.0052
056-Mo	0.10	0.36	0.023	0.009	0.019	0.022	0.001	0.38	0.39	0.056	0.0038

the microstructure is composed of polygonal ferrite (FP) with less acicular ferrite (FAc) and bainite (B). In this case, the higher surface energy of the grain boundaries favors the formation of polygonal ferrite and limits the growth of bainite plates^{21,23,25,26}.

Figure 3 shows the microstructural characteristics after quenching and tempering at 450 and 600 °C, where FP, B

and FAc represent polygonal ferrite, bainite and acicular ferrite, respectively.

In Figure 3(a), elongated bainite slabs (B) predominate in 160-Mo steel. In 056-Mo steel, Figure 3(b) shows acicular ferrite (FAc) and bainite in a polygonal ferrite (FP) matrix after tempering at 450 °C. Figures 3(c) and 3(d) show that, after tempering at 600 °C, both steels remain with ferritic-

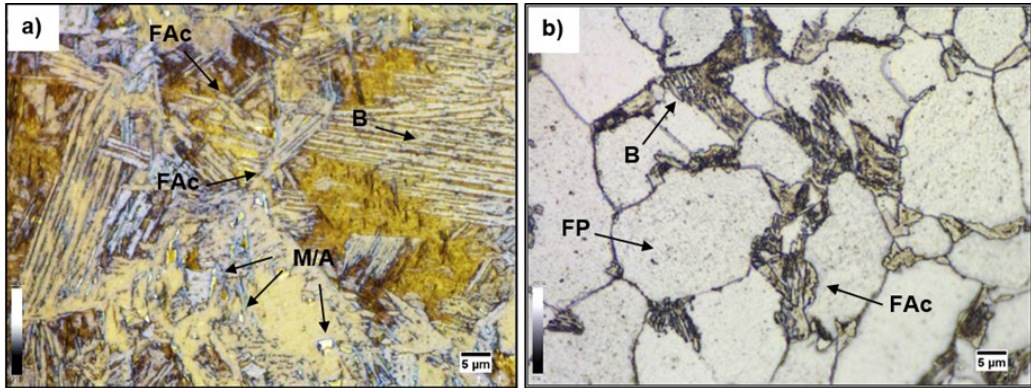


Figure 2. Quenching at 900 °C. (a) Acicular ferrite, elongated bainite plates and M/A in 160-Mo steel (Lepera - MOC); (b) polygonal ferrite, acicular ferrite and bainite in 056-Mo steel (Nital 2% - MOC).

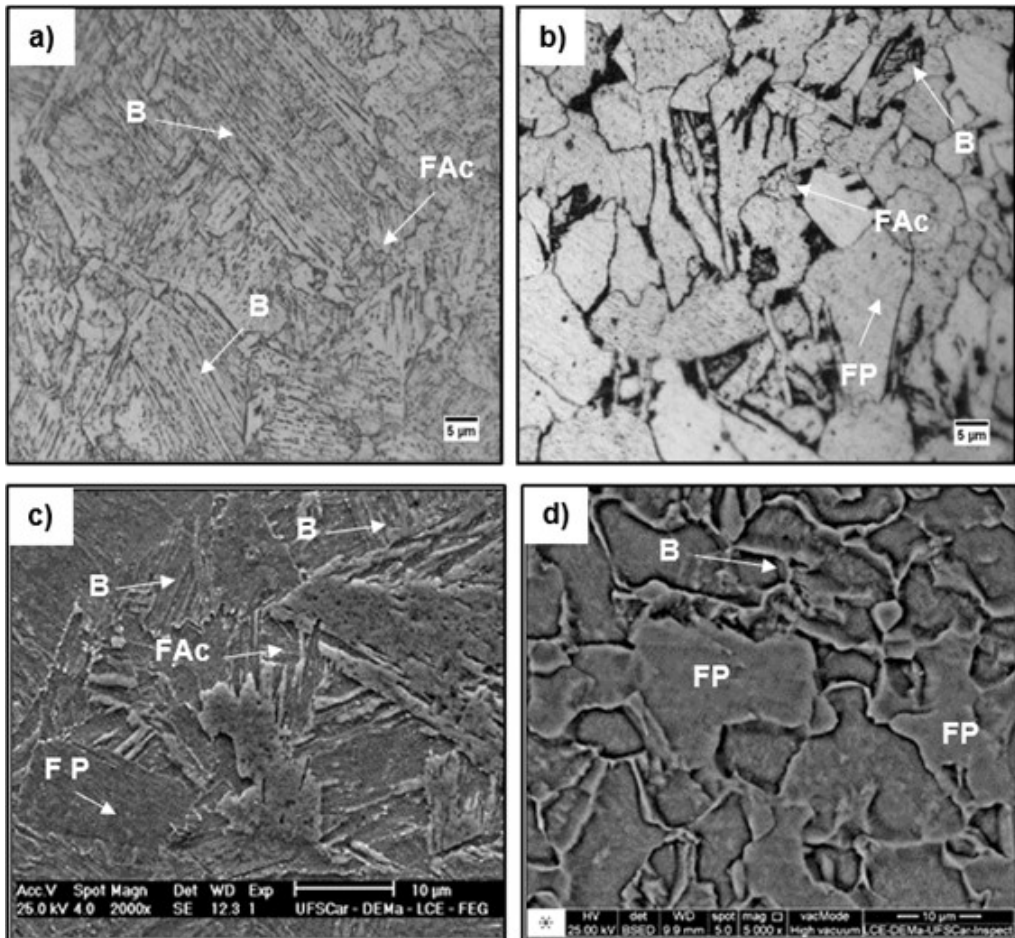


Figure 3. (a) and (c) 160-Mo after tempering at 450 and 600 °C. (b) and (d) 056-Mo after tempering at 450 and 600 °C (MOC and SEM – Nital 2%).

bainitic microstructures, but with an increase in the amount of polygonal ferrite. According to literature, niobium and molybdenum favor this microstructure after tempering^{10,25}.

On the tempering curves in Figure 4, initially there is a relief of the stresses generated in the quenching. The greater hardness of 160-Mo steel is related to the higher molybdenum content and the presence of displacive constituents and elongated bainite bundles⁸. Previous studies with Nb-Mo containing HSLA steels indicate, that the addition of Mo promotes the formation of bainite with excellent mechanical properties^{8,11}. Probably the effect of secondary hardening is responsible for the increase in hardness in the range from 400 to 500 °C²⁷. In this case, molybdenum should contribute to the precipitation mechanism of finely distributed carbides in the matrix^{14,28}. According to Isasti, these carbides in the

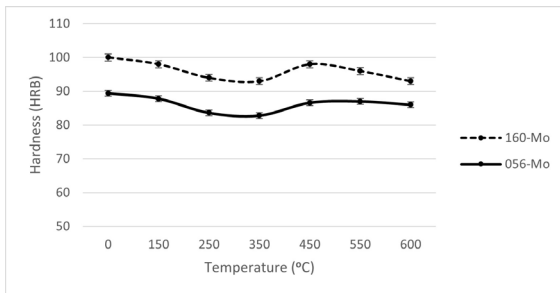


Figure 4. Hardness values as a function of tempering temperature. Average of five measurements for each condition.

order of 15 nm increase the hardness and yield strength in microalloyed steels¹⁴. Wang et al. observed a hardening of the ferritic phase in a steel microalloyed with titanium and molybdenum and attributed the reinforcement to the nanometric precipitation of carbides. After tempering at temperatures above 500 °C the hardness gradually decreases²⁹.

This is due to the coalescence of carbides shown in Figure 5(a) in 160-Mo steel after quenching at 900 °C and tempering at 600 °C. The EDS spectrum in Figure 5(b) indicates the particles of molybdenum carbides.

Fine particles from secondary precipitation are difficult to see by scanning electron microscopy. However, the results shown in Figure 5(a) and Table 2 indicate secondary hardening and coalescence of carbides in this temperature range. Regarding the mechanical properties of 160-Mo steel, it is possible that the effect of molybdenum is greater on the microstructure, as shown in Figure 2(a), than on secondary hardening.

According to values of mechanical properties, in Table 2, the presence of bainite plates is more important in 160-Mo steel and favors higher values of yield strength and ultimate tensile strength, and secondary hardening is negligible. However, in 056-Mo steel, there is a greater influence of the secondary hardening mechanism^{30,31}. In this case, molybdenum reduces the interfacial energy of the precipitates and decreases the coalescence rate of niobium carbides³².

After tempering at 600 °C of 160-Mo steel, the lowest yield strength and the highest elongation values indicate a possible decomposition of M/A, the thickening of bainite plates and carbides coalescence. Talebi observed the beginning

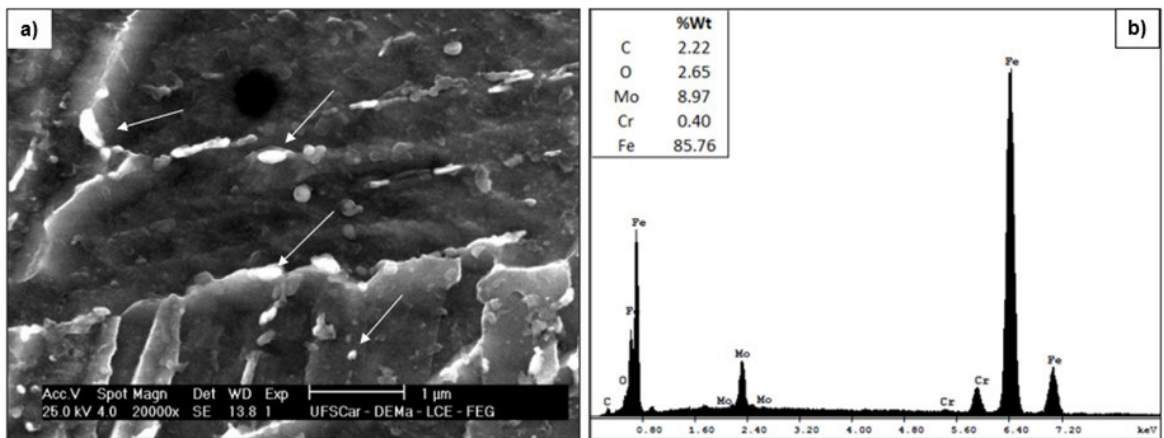


Figure 5. (a) and (b) Steel 160-Mo after quenching 900 °C and tempering 600 °C: particles of molybdenum carbides indicated by the arrows and the spectrum of concentrations obtained with the analysis by EDS (Nital 2% - SEM).

Table 2. Average values of yield strength (σ_y), ultimate tensile strength (σ_t), percentage elongation (% E) and the absorbed energies in the Charpy impact test at -20 °C (Q – Quenching and T – tempering).

	Treatment	σ_y (MPa)	σ_t (MPa)	% E	Energy (J)
160-Mo	T 900	672 ± 12	934 ± 05	9 ± 1	10 ± 2
160-Mo	T 900 + R 450	563 ± 10	628 ± 14	8 ± 1	13 ± 1
160-Mo	T 900 + R 600	544 ± 05	609 ± 06	15 ± 1	8 ± 1
056-Mo	T 900	302 ± 10	507 ± 05	24 ± 2	365 ± 15
056-Mo	T 900 + R 450	337 ± 05	433 ± 07	29 ± 2	382 ± 11
056-Mo	T 900 + R 600	410 ± 08	502 ± 13	24 ± 3	171 ± 13

M/A decomposition in tempering at 350 °C and complete decomposition at 600 °C in bainitic steels³³.

Regarding impact resistance, the elongated bainite plates and the presence of the embrittlement microconstituent M/A, shown in Figure 2(a), justify the reduction in absorbed energy in the 160-Mo steel^{34,35}. However, in 056-Mo steel, the behavior is different, as, according to Figure 2(b). In this case, the amount of bainite and M/A is not significant compared to 160-Mo steel and the values of yield strength and ultimate tensile strength are lower. Thus, an increase in ductility and impact energy is possible. Another important factor, observed in the same figure, is the presence of polygonal ferrite associated with acicular ferrite and granular bainite, which contribute to toughness increasing. Experimental results show that this microstructure improves yield strength and toughness of ferrite-base steels³⁶.

In 056-Mo steel, although it is not possible to confirm, the increase in yield strength and ultimate tensile strength may be related to the secondary hardening mechanism that can occur in the range of 450 to 600 °C, as seen in Figure 4.

From this perspective, the thermodynamic simulations with the ThermoCalc software in Figures 6 and 7 corroborate the results, because indicate a larger amount of complex carbides in the steels, in the range of 400 to 600 °C. Literature shows

that M_7C_3 and $M_{23}C_6$ carbides are mainly chromium and molybdenum. These carbides, with complex stoichiometry, form a coarse dispersion^{15,37}. Dong et al. also observed different precipitates during tempering: M_3C_2 between 200 and 400 °C, M_2C and $M_{23}C_6$ at 500 °C in ultra-high strength steels³⁸. Thus, the greater amount of precipitates of $M_{23}C_6$ in the range of 400 to 600 °C may indicate an increase in mechanical strength and a reduction in absorbed energy on impact in 160-Mo steel.

Finally, the API 5L standard specifications can validate the results of mechanical properties. Regarding the chemical composition and mechanical properties, according to quenching at 900 °C and tempering at 600 °C for the two steels, and using Equation 1 to calculate the elongation, the 056-Mo steel fits at PSL 2 level, while 160-Mo steel at PSL 1 level¹³.

$$A_f = C \frac{A_{xc}^{0,2}}{U^{0,9}} \quad (1)$$

According to yield strength (σ_y) and the ultimate tensile strength (σ_t) in Table 2, the 056-Mo steel can be considered as API X65 grade, while 160-Mo steel as X70. With relation the absorbed energy, it is observed that the 056-Mo steel meets the standard value and the fracture is fully ductile. However, 160-Mo steel does not have the minimum value of 27 Joules and has a high percentage of brittle fracture.

4. Conclusions

The results show that:

- Molybdenum favors the formation of elongated plates of bainite, which increases mechanical strength and reduces toughness;
- The smallest grain size and the largest amount of polygonal ferrite increase the absorbed energy in the 056-Mo steel;
- Simulations with ThermoCalc software indicate a higher precipitation of carbides in 160-Mo steel and corroborate the results of mechanical properties;
- Qualitative analyzes of chemical composition by EDS, associated with the tempering curves, indicate the presence of the secondary hardening mechanism and carbides coalescence;
- According to API 5L standard, 056-Mo steel is similar to PSL 2, X65 grade, while 160-Mo is similar to PSL 1, X70 grade. However, the absorbed energy in the impact test for the second do not meet the minimum value required by the standard.

5. Acknowledgments

The authors thank Grupo Metal for the samples, CAPES for master's scholarship from student Jaqueline, CBMM for niobium, LCE/UFSCar for the analysis, FAPES for the financial support, IFES by the use of equipments and MSc. Joelma Krugel for thermodynamic simulations.

6. References

1. Gray JM, Siciliano F. High strength microalloyed linepipe: half a century of evolution. Houston: Microalloyed Steel Institute; 2009.

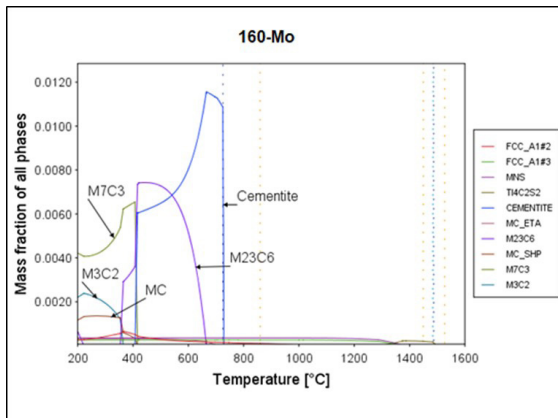


Figure 6. Thermodynamic simulation performed on steel 160-Mo: MC, M_3C_2 , M_7C_3 and $M_{23}C_6$ carbides.

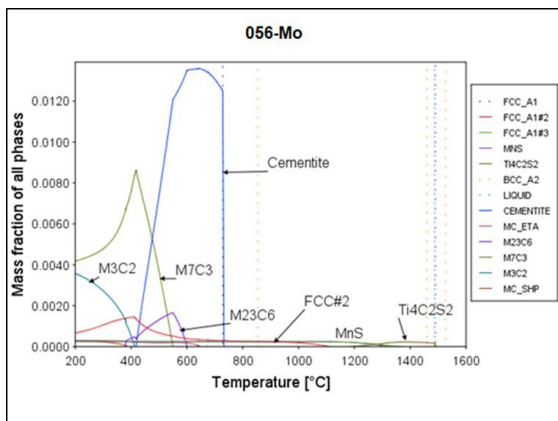


Figure 7. Thermodynamic simulation performed on steel 056-Mo: MC, M_3C_2 , M_7C_3 and $M_{23}C_6$ carbides.

2. Kumar BVR. A review on importance of microalloying in steel. *Int J Mech Eng.* 2014;5(2):187-93.
3. Forged Components [internet]. Forging types API wellhead component manufacturing. Navasota: Forged Componentes; 2021 [cited 2021 Feb 28]. Available from: https://forgedcomponents.com/forging-types-api-wellhead-component-manufacturing_2017-10/.
4. Speer JG, Matlock DK. Some recent developments in microalloyed bar and forging steels. new developments in long and forged products proceedings. Warrendale: AIST; 2006.
5. Speer JG, Whitley B, Kaster S, Findley K, Matlock D, Moor E. Selected developments in Nb-microalloyed forgings for induction hardening, and pearlitic wire rod. *Tecnol Metal Mater Min.* 2020;17(2):164-9.
6. Fatehi A, Calvo J, Elwazri AM, Yue S. Strengthening of HSLA steels by cool deformation. *Mater Sci Eng A.* 2010;527:4233-40.
7. Mousavi ASH, Yue S. The effect of cooling rate, and cool deformation through strain-induced transformation, on microstructural evolution and mechanical properties of microalloyed steels. *Metall Mater Trans, A Phys Metall Mater Sci.* 2012;43:1140-62.
8. Mousavi ASH, Sabzi M. The Evolution of Microstructure of an High Ni HSLA X100 Forged Steel Slab by Thermomechanical Controlled Processing. In: 147th Annual Meeting & Exhibition Supplemental Proceedings; 2018 Feb 4. Cham: Springer; 2018. p. 145-56.
9. Okaguchi S, Hashimoto T, Ohtani H. Effect of niobium, vanadium and titanium on transformation behavior of hsla steel in accelerated cooling. In: International Conference on Physical Metallurgy of Thermomechanical Processing of Steels and Other Metals; 1988 June 6-10; Tokyo: THERMEC; 1988. p. 330-6.
10. Shang CJ, Miao CL, Subramanian SV. Austenite processing and phase transformation of niobium and molybdenum alloyed high performance structural steel. In: Fundamentals and Applications of Mo and Nb Alloying in High Performance Steels; 2014 April 24-26; Pittsburgh. Pittsburgh: CBMM, IMO, TMS; 2014. v. 1, p. 37-61.
11. Huang BM, Yang JR, Huang CY. The synergistic effect of niobium-molybdenum additions on the microstructure of low-carbon bainitic steel. In: Fundamentals and Applications of Mo and Nb Alloying in High Performance Steels; 2013 April 24-26; Pittsburgh. Pittsburgh: CBMM, IMO, TMS; 2013. v. 2, p. 29-50.
12. Li L, Xu L. Designing with High-Strength Low-Alloy Steels. In: Totten GE, Xie L, Funatani K, editors. *Handbook of Mechanical Alloy Design.* New York: Marcel Dekker; 2004. p. 249-320.
13. API: American Petroleum Institute. Specification 5L for line pipe. 45th ed. Washington DC: API; 2013.
14. Isasti N, Jorge-Badiola D, Taheri ML, Uranga P. Phase transformation study in Nb-Mo microalloyed steels using dilatometry and EBSD quantification. *Metall Mater Trans, A Phys Metall Mater Sci.* 2013;44(8):3552-63.
15. Han Q, Kang Y, Zhao X, Gao L, Qiu X. High-temperature properties and microstructure of Mo microalloyed ultra-high-strength steel. *Int J Miner Metall Mater.* 2011;18(4):407-13.
16. Xu K, Thomas BG, O'Malley R. Equilibrium model of precipitation in microalloyed steels. *Metall Mater Trans, A Phys Metall Mater Sci.* 2010;42(2):524-39.
17. Kasatkin OG, Vinokur BB, Pilyushenko VL. Calculation models for determining the critical points of steel. *Metal Sci Heat Treat.* 1984;26(1):27-31.
18. Javaheri V, Khodaie N, Kajjalainen A, Porter D. Effect of niobium and phase transformation temperature on the microstructure and texture of a novel 0.40% C thermomechanically processed steel. *Mater Charact.* 2018;142:295-308.
19. Coladas J, Masounave J, Bailon JP. The influence of niobium on the austenite processing of medium and high carbon steels. In: Balance JB, editors. *The hot deformation of austenite.* New York: AIME; 1977. p. 341-88.
20. Mori FY, Barbosa CA, Souza MHC, Falleiros IGS. Controle do tamanho de grão austenítico de um aço para trabalho a quente através de adição de Nb. *Meturgia ABM.* 1977;33(241):743-8.
21. Haijiang H, Guang X, Li W, Zhengliang X, Yulong Z, Guanghui L. The effects of Nb and Mo addition on transformation and properties in low carbon bainitic steels. *Mater Des.* 2015;84:95-9.
22. Feng H, Kaiming W, Ting-Ping H, Peter H, Rodionova I, Fu-Cheng Z. The effect of microphases on elongation of nanostructured bainitic steels. *Metallurgist.* 2017;60(11-12):1295-300.
23. Bhadeshia HKDH, Edmonds DV. The bainite transformation in a silicon steel. *Metall Trans, A, Phys Metall Mater Sci.* 1979;10(7):895-907.
24. Isasti N, Jorge-Badiola D, Taheri ML, Uranga P. Microstructural features controlling mechanical properties in nb-mo microalloyed steels. Part II: impact toughness. *Metall Mater Trans, A Phys Metall Mater Sci.* 2014;45A:4972-82.
25. Bhadeshia HKDH. *Bainite in steels.* 2nd ed. London: Institute of Materials; 2001.
26. Shin SY, Hwang B, Lee S, Kim NJ, Ahn SS. Correlation of microstructure and charpy impact properties in API X70 and X80 line-pipe steels. *Mater Sci Eng A.* 2007;458:281-9.
27. Ma YQ, Gao HT, Liang YF, Zhang XJ. Secondary hardening during tempering of Cr-W-Mo-V high alloy medium-upper carbon steel and its hardness forecast. *Adv Mat Res.* 2011;415-417:813-8.
28. Porter DA, Easterling KE, Sherif M. *Phase transformations in metals and alloys.* 3 ed. Londres: CRC Press; 2009.
29. Wang J, Beladi H, Pan L, Fang F, Hu J, Kong L, et al. Interphase precipitation hardening of a Ti-Mo microalloyed dual-phase steel produced by continuous cooling. *Mater Sci Eng A.* 2021;804:140518.
30. Davis JR. *Alloying: understanding the basics* In: Davis JR, editor. *Materials park.* Ohio: ASM International; 2001.
31. Aluna MA, Iza-Mendia A, Gutiérrez I. Precipitation of Nb in ferrite after austenite conditioning. Part II: strengthening contribution in High-Strength Low-Alloy (HSLA) steels. *Metall Mater Trans, A Phys Metall Mater Sci.* 2012;43:4571-86.
32. Abbasi E, Rainforth WM. Effect of Nb-Mo additions on precipitation behaviour in V microalloyed TRIP-assisted steels. *Mater Sci Technol.* 2016;32(16):1721-9.
33. Talebi S, Jahazi M, Melkonyan H. Retained austenite decomposition and carbide precipitation during isothermal tempering of a medium-carbon low-alloy bainitic Steel. *Materials.* 2018;11(8):1441.
34. Junhua K, Lin Z, Bin G, Pinghe L, Aihua W, Chandsheng X. Influence of Mo content on microstructure and mechanical properties of high strength pipeline steel. *Mater Des.* 2004;25:723-8.
35. Shen YF, Qiu LN, Sun X, Zuo L, Liaw PK, Raabe D. Effects of retained austenite volume fraction, morphology, and carbon content on strength and ductility of nanostructured TRIP-assisted steels. *Mater Sci Eng A.* 2015;636:551-64.
36. Kim YM, Kim SK, Lim YJ, Kim NJ. Effect of microstructure on the yield ratio and low temperature toughness of linepipe steels. *ISIJ Int.* 2002;42(12):1571-7.
37. Maalekian M. *The effects of alloying elements on steels (I)* [thesis]. Graz: Technische Universität Graz; 2007.
38. Dong J, Zhou X, Liu Y, Li C, Liu C, Guo Q. Carbide precipitation in Nb-V-Ti microalloyed ultra-high strength steel during tempering. *Mater Sci Eng A.* 2017;683:215-26.